Linearity characterization of a dual-parallel Mach-Zehnder modulator

Yanyang Zhou, Linjie Zhou*, Shen Liu, Haike Zhu, Minjuan Wang, Xinwan Li and Jianping Chen
State Key Laboratory of Advanced Optical Communication Systems and Networks, Department of Electronic Engineering, Shanghai Jiao Tong University, Shanghai 200240, P.R. China
**ljzhou@sjtu.edu.cn*

Abstract: We achieve highly-linear modulation by using two parallel simultaneously-driven Mach-Zehnder modulators. Measurement results show that the third-order intermodulation distortion is suppressed significantly.

OCIS codes: (250.4110) Modulator; (230.2090) Electro-optical devices;

1. Introduction.

Silicon photonics are one of the most suitable platform for the microwave photonic (MWP) links due to its low cost, high energy efficiency and high bandwidth. An optical modulator converts a radio-frequency (RF) signal from the electrical domain to the optical domain with its linearity being one of the most important performance metrics in MWP links. The carrier-depletion-based silicon Mach-Zehnder modulators (MZMs) exhibit high performances in terms of modulation speed and link robustness. However, compared with $LiNbO_3$ MZMs where the linear electro-optic effect is used, the silicon MZMs are realized based on the free-carrier dispersion (FCD) effect, leading to the nonlinear response of phase shift to drive voltage and therefore more harmonic and intermodulation distortions. These distortions limit the spurious-free dynamic range (SFDR) of the MWP links. Many modulator configurations have been proposed to increase the SFDR, such as the push-pull drive scheme [1], the ring-assisted Mach-Zehnder interferometer (RAMZI) structure [2], and the dual-parallel MZM structure [3].

In this work, we present the linearity measurement in a dual-parallel MZM consisting of two carrier-depletion-based silicon modulators with a single-drive push-pull travelling wave electrode (TWE) configuration. Compared with the single MZM, the ratio of intermodulation to carrier is significantly reduced for the dual-parallel MZM. The SFDRs for the third-order intermodulation distortion ($SFDR_{IMD}$) are 101.41 dB·$Hz^{2/3}$ and 94.17 dB·$Hz^{2/3}$ at 1 GHz and 15 GHz RF frequencies, respectively.

2. Device principle and structure

Fig. 1(a) shows the structure of the dual-parallel MZM consisting of two nested MZMs. The top child MZM works as the primary modulator with its bias at a quadrature point. The bottom child MZM works as the secondary modulator with its bias at a quadrature point π phase different from the point chosen for the primary modulator. The input optical power is higher in the primary modulator while its RF drive power is lower. In this way, by properly choosing the ratios of both the input optical power and the RF power for the two modulators, the third-order distortions from the primary and secondary modulators can be cancelled, while the fundamental signal power only suffers a slight reduction.

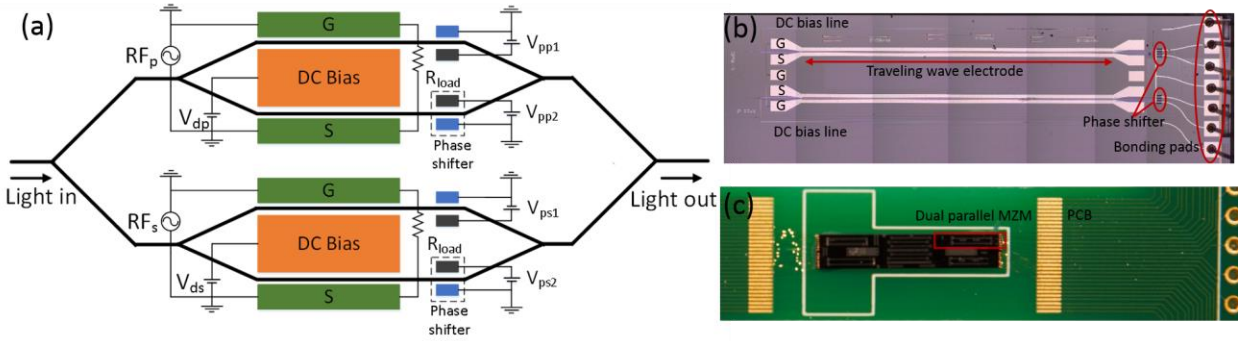

Fig. 1. (a) Device structure of the dual-parallel MZM. (b) Microscope image of the MZM. (c) Device photo after wire-bonding to a PCB.

In our device design, each child MZM contains a 3-mm-long single-drive push-pull TWE connecting to the heavily p^+-doped regions, a DC bias electrode connecting to the heavily n^+-doped region and two 50-μm-long

thermo-optic phase shifters. In order to achieve a high electro-optical bandwidth and high thermal tuning efficiency, the TWE and the phase shifters are optimized respectively [4, 5]. The fabrication was done using the IME standard CMOS process. Figure 1(b) shows the microscope image of the fabricated device. The footprint of our device is 4.77 mm × 1.35 mm. The DC bias line and thermo-optic phase shifters are connected to a printed circuit board (PCB) through wire bonding. Fig. 1(c) shows the photo of the chip after wire-bonding to a PCB.

3. Experimental results

Fig. 2 shows the experimental setup. A two-tone RF signal generated by the vector network analyzer (VNA) is split into two halves and amplified to drive the dual-parallel MZM via a 40-GHz-bandwidth microwave GSGSG probe. The other ends of the TWEs are terminated with two external 50-ohm resistors via another GSGSG probe. Voltages are applied to the phase shifters and DC biases through the PCB. Input light from a continuous wave tunable laser goes through a polarization controller to set the transverse electric (TE) polarization and is then coupled to the MZM through an on-chip inverse taper. To measure the optical spectrum, the modulated output optical signal is connected to an optical spectrum analyzer (OSA). Alternatively, the output signal is amplified by an erbium-doped fiber amplifier (EDFA) followed by an optical filter before received by a photodiode. The converted electrical signal is finally fed back to the VNA for RF spectrum and SFDR measurements.

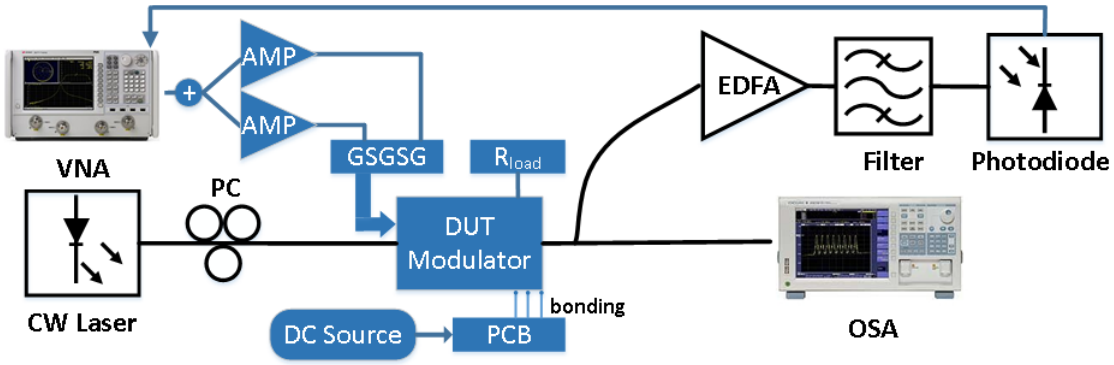

Fig. 2. Experimental setup to measure the linearity of the dual-parallel MZM.

For the linearity measurement, we set the two frequency tones at 14.995 GHz and 15.005 GHz. The proper ratio of the RF power to drive the primary and secondary modulators is obtain by adjusting the gain of the two RF amplifiers. In our measurement, the RF powers driving the primary and secondary modulators are 16.3 dBm and 20 dBm, respectively. In order to set the proper optical power for the two modulators, we apply different DC bias voltages onto the two child modulators (V_{dp} = 8 V and V_{ds} = 2.4 V). Because the width of the carrier depletion region varies with bias voltage, the optical loss is different for each modulator. The modulation operation point is set by tuning the phase shifters (V_{pp1}, V_{pp2}, V_{ps1}, and V_{ps2}). The output signal from the child modulator has harmonic distortions because of the nonlinear response of phase shift and optical loss to voltage. Figs. 3(a) and 3(b) show the output optical spectra when either the primary or the secondary modulator is driven by the RF signal. High-order harmonic components are clearly observed in the measured optical spectra. When the two child modulators are driven simultaneously, the high-order components are highly suppressed with 11.5 dBm suppression ratio for the 2nd and 6.7 dBm for the 3rd harmonic components, as shown in Fig. 3(c).

Figs. 3(d)-3(e) show the measured RF spectrum indicating the relative magnitude of the fundamental and the IMD. The RF powers are 12.6 dBm and 17.9 dBm for the primary and secondary modulators, respectively. The photodetector current is 1.7 mA with a responsivity of 0.5 A/W. The whole electrical links including coaxial cables and microwave probes are calibrated prior to the measurement. Compared to the primary MZM, the dual-parallel MZM exhibits an IMD reduced by 10.2 dBm while the fundamental is only lowered by 1.5 dBm.

Fig. 4 shows the IMD to carrier ratio (dBc.IMD) versus input RF power for the primary and dual-parallel MZMs. The RF frequencies are set at 15 GHz (14.995 GHz and 15.005 GHz) and 1 GHz (1005 MHz and 995 MHz) bands for two measurements. Comparing the two traces at 15 GHz, the dBc.IMD is reduced by 18.5 dB for the dual-parallel MZM. The calculated $SFDR_{IMD}$ for the dual-parallel MZM is 94.17 dB $Hz^{2/3}$ with the noise floor of 161 dBm. When the RF frequency is set around 1 GHz, the dBc.IMD is reduced by 19.4 dB. The calculated $SFDR_{IMD}$ is 101.41 dB $Hz^{2/3}$.

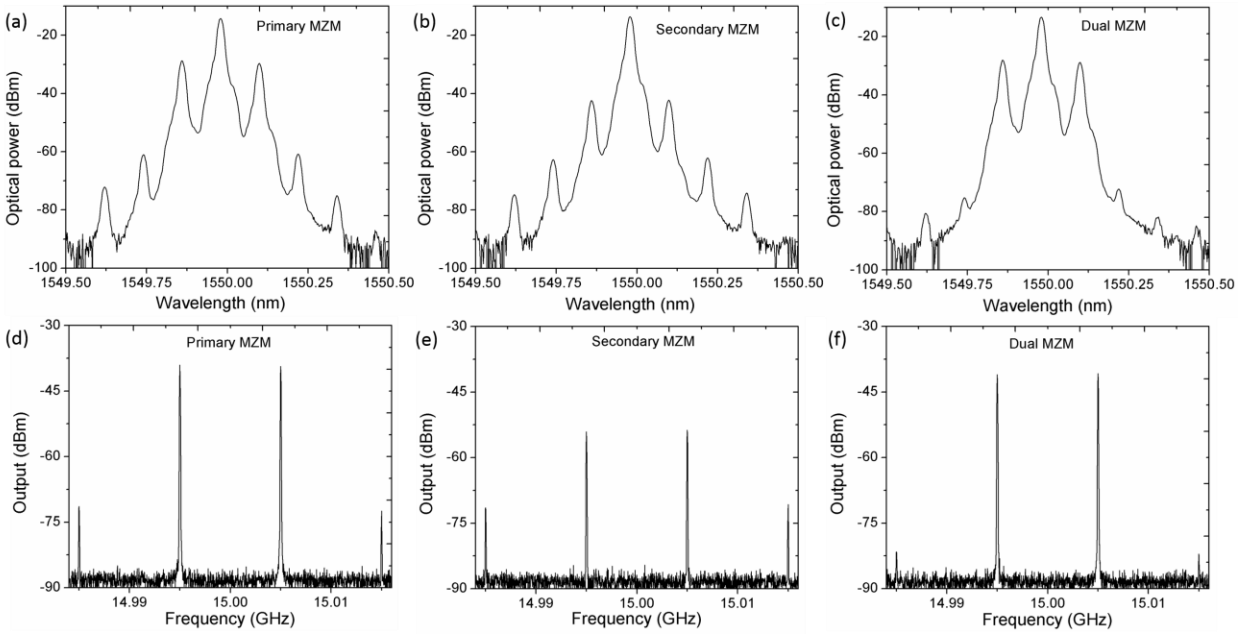

Fig. 3. (a)-(c) Output optical spectra measured by the OSA. (d)-(f) Output RF spectra showing the fundamental and the third-order intermodulation measured by the VNA. (a) and (d): Primary MZM; (b) and (e): Secondary MZM; (c) and (f): Dual-parallel MZM.

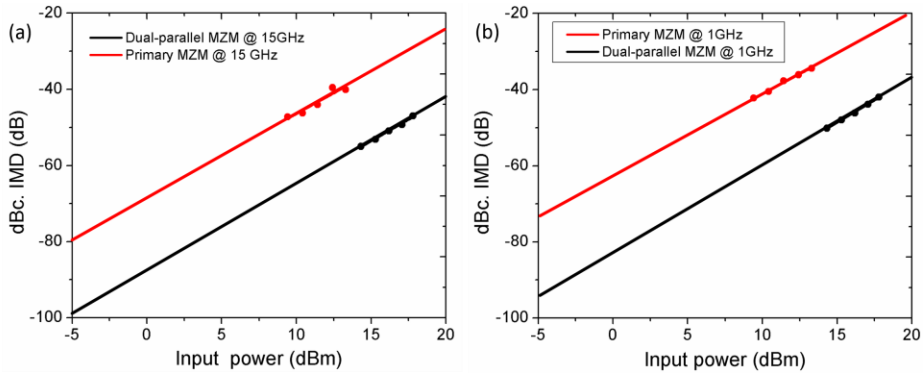

Fig. 4. IMD to carrier ratio versus input RF power for the primary and dual-parallel MZMs with the RF frequencies around (a) 15 GHz and (b) 1 GHz. The dots represent the measured data and the lines are the linear fitting.

4. Conclusion

We have presented an experimental measurement of the linearity of a silicon dual-parallel MZM driven by push-pull single-drive TWEs. With a proper choice of RF power, bias voltage and operation point for the primary and secondary modulators, the third-order intermodulation distortion can be partially canceled. The ratio of IMD to carrier is effectively suppressed in the dual-parallel MZM with the $SFDR_{IMD}$ being 94.17 dB·$Hz^{2/3}$ and 101.41 dB·$Hz^{2/3}$ at 15 GHz and 1 GHz RF frequency bands, respectively.

5. References

[1] M. Streshinsky, A. Ayazi, Z. Xuan, A. E.-J. Lim, G.-Q. Lo, T. Baehr-Jones, et al., "Highly linear silicon traveling wave Mach-Zehnder carrier depletion modulator based on differential drive," *Opt. express*, vol. 21, pp. 3818-3825, 2013.
[2] J. Cardenas, P. A. Morton, J. B. Khurgin, A. Griffith, C. B. Poitras, K. Preston, *et al.*, "Linearized silicon modulator based on a ring assisted Mach Zehnder inteferometer," *Opt. express*, vol. 21, pp. 22549-22557, 2013.
[3] J. L. Brooks, G. S. Maurer and R. A. Becker, "Implementation and evaluation of a dual parallel linearization system for AM-SCM video transmission," *J. Light. Technol*, vol. 11, pp. 34-41, Jan. 1993.
[4] J. Wang, L. Zhou, H. Zhu, R. Yang, Y. Zhou, L. Liu, T. Wang, and J. Chen, "Silicon high-speed BPSK modulator with a single-drive push-pull high speed travelling wave electrode", *Photon. Res.* vol. 3, no. 3, pp. 58-62, Jun. 2015.
[5] Q. Wu, L. Zhou, X. Sun, H. Zhu, L. Lu and J. Chen, "Silicon thermo-optic variable optical attenuators based on Mach–Zehnder interference structures," *Opt. Commun.*, vol. 341, pp. 69–73, Dec. 2015.